Titanium dioxide layer deposited at low temperature upon polyester fabrics

I. ZGURA[*], S. FRUNZA, L. FRUNZA, M. ENCULESCU,
C. FLORICA, C. P. GANEA, C. C. NEGRILA, L. DIAMANDESCU
National Institute of Materials Physics, PO Box Mg 07, 077125 Magurele, Romania

TiO_2 deposition by sputtering or sol-gel techniques was applied onto less thermal stable polyester textiles and onto a related poly(lactic acid) material. The temperature of deposition and of the further treatment was low enough as allowed by the support nature. Structural and spectroscopic characterization of the raw and coated samples has been performed. TiO_2 coated particles are amorphous as indicated by X-ray diffraction and scanning electron microscopy. Sputtered layers consist in aggregates randomly distributed on the substrate while the sol gel layers show a uniform coverage of nanoparticles having a mosaic-like structure. The morphology of the sputtered layers depends on the deposition pressure as well. The loading degree estimated on the basis of the thermogravimetric data is rather low (ca. 2%), but the fabric properties are much influenced by the deposition. Photocatalytic activity also present on the coated surfaces was evaluated in the methylene blue degradation. TiO_2 layer is quite adherent as checked by an ultra-sonication method.

1. Introduction

Titanium dioxide TiO_2 (titania) is a transition metal oxide with UV absorbing properties which are very interesting not only from a scientific standpoint but also due to technological applications in many fields [1]. There are three features of titanium dioxide, which make its photocatalytic properties, such as high photocatalytic efficiency, great stability and low cost of production [2]. In addition to bulk applications, TiO_2 thin layers were obtained upon different materials for UV blocking, antibacterial or/and photo catalytic properties.

TiO_2 coating of the fibers can be performed by several techniques, such as sputtering [3-6] ion beam evaporation [7] plasma enhanced chemical vapor deposition [8-11], sol-gel [12] (dip-)pad-dry-cure [13-16], impregnating TiO_2 particles in a resin and this composite deposited into the yarn-array [17]. Due to their low thermal stability, polyester (PES) fibers should be covered at lower temperature; then covering methods used deposition temperature lower than for natural fibers [18-22]. In some cases, specific pretreatments were applied using polysiloxane [23], citric acid [24], aminopropyl trimethoxysilane [25] or enzymatic modification [26,27], impregnation with peroxo titanic acid solution [28], hydrolysis of $TiCl_4$ in the presence of nanocrystalline cellulose grafted fabric [29], or attachment of nanocrystalline titania nanoparticles codissoluted in isopropanol and chloroform [30].

The aim of this work was to test the possibilities of deposition of titanium oxide particles onto the surface of polyester fabrics leading to modified properties, e.g. to photocatalytic ones. Our polyester textiles have different mesh sizes [31] and fabrication mode. In addition, samples of poly(lactic acid) (PLA) were considered; this compound is related to PES due to the presence of carboxy groups. An important issue was to obtain a good binding of the oxide particles to this rough surface. Two methods for TiO_2 deposition at low temperature were chosen, methods which were applied with different results onto glass substrates [32]. We found that TiO_2 deposition was possible onto polyester fabrics at low temperature by both techniques and that the deposition leads to amorphous oxide particles. In fact amorphous layers are rarely mentioned [32,33] even though TiO_2 can be used for coating without heating.

For testing TiO_2 adhesion a technique of treating the surface of the coated textiles with ultrasound waves [34] was used. Besides, UV photocatalytic degradation of methylene blue in the presence of coated fabrics was evaluated as well using a PCC2 Photocatalytic Checker.
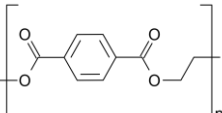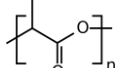
2. Experimental

2.1 Fabric samples

The investigated textiles were commercially purchased; they differ by the chemical nature of the fibers and by the surface roughness given by the manufacturing mode (see Table 1).

Prior to functionalization the plain weave was cut at the dimensions of ~20×20 mm and washed in n-propylic alcohol by 5 min sonication to remove the impurities. The drying was performed at room temperature in a laminar flow hood to avoid the dust.

Table 1 Textiles investigated for TiO$_2$ deposition

Sample label	Textile 2D-element/ thread *	Nature/formula of the fibers	Thickness [mm]	Density [g/cm^3]	Color
PES2	Knitted/ interlock/Nm 70/1	Polyester/	0.82	0.25	White
PES3	Knitted/ interlock/Nm 50/1		0.89	0.26	White
PES28	Fabric warp Nm 70/2/ weft Nm 70/2		0.46	0.47	White
PES30	Fabric warp Nm 70/2/ weft Nm 40/2		0.52	0.41	White
PLA	Non-woven	Poly(lactic acid) /	0.64	0.31	White

* Warp - the longitudinal threads; weft - the lateral threads. Nm means length in meters per 1g mass.

2.2. Surface functionalization

Textile surface was modified with TiO$_2$ by two deposition techniques, sputtering and sol-gel. This modification leading to changed surface properties was further called functionalization.

- Sputtering (SP) deposition used a Sputter-Coater (Tectra GmbH) installation and a TiO$_2$ target (99.9% oxide, K.J. Lesker). Deposition time (kept in all the experiments) was 6 h at three pressures: 4×10^2 Pa, 8.6×10^2 Pa (most of the samples) and even 4×10^3 Pa, though the free mean path was too low in this case for a good deposition. The distance sample-target was kept constant for all the experiments. The incident beam was obtained at 200 W constant power under argon plasma. The sample was processed at room temperature.

- Sol-gel (SG) deposition was performed by covering the fabrics with TiO$_2$ by dip coating from a TiO$_2$ sol in a home made installation at a drawing rate of 10 mm/min. As precursor for TiO$_2$ sol synthesis was used titanium(IV) tetraisopropoxide (TIP) (Sigma Aldrich). TiO$_2$ sol was prepared by stirring (300 rpm) for 2h at room temperature, the following reaction mixture: ethylic alcohol (abs., Sigma Aldrich) 31.15 ml; acetic acid (glacial, Sigma Aldrich) 17.15 ml; TIP 13.4 ml; chlorhydric acid (conc., Alfa Aesar) 0.153 ml.

In some cases, TiO$_2$ layers were coated onto (cleaned) glass plates at the same time with the textile samples.

Sample notation retains the treatment applied: the original samples keep the material label of Table 1 for the 'substrate' while functionalized samples are noted TiO$_2$SPn/substrate or TiO$_2$SG/substrate where 'substrate' is either a textile material or a glass plate. "n" is the number of 10^2 Pa in the deposition chamber; thus TiO$_2$SP8.6/PES2 means that the sputtering took place at 8.6×10^2 Pa.

Once obtained the coated surfaces, the adherence of the layer was checked by submitting the coated samples to a sonication treatment for 3 min or for 1h in an equipment UIS250V (Hilscher Ultrasound Technology) of max. 250 W in a continuous mode at 70% amplitude. The sample immersed in water was very close to the resonant horn.

2.3. Characterization

Both the original and the coated fabrics were characterized by applying the following techniques:

- X-ray diffraction (XRD) studies with a D8 Advance equipment (Bruker-AXS) with a CuK$_\alpha$ radiation (K$_\beta$ radiation being eliminated using a nickel filter) allowed phase identification.

- X-ray photoelectron spectroscopy (XPS) of the elemental composition of the fabric surface with an electron spectrophotometer SPECS, a Phoibos 150 analyzer and a XR-50M source operating on Al monochromatic anode (E$_x$=1486.7 eV) at 300 W, 24 mA and 12.5 kV. Charge was compensated with a flood gun FG15/40. Pass energy was 20 eV for high resolution narrow spectra and 50eV for the extended spectra. The data were fitted with Voigt function by the Spectral Data Processor 2.3 program.

- Scanning Electron Microscopy (SEM) performed with a Zeiss Evo 50 XVP instrument after conventional gold metallization of the samples.

- Thermogravimetric measurements (TG) performed with a Diamond TG-DTA apparatus (Perkin Elmer) in a temperature range from room temperature to 1050 K, at a heating rate of 10 Kmin^{-1}. The textile samples were carefully chopped and added to the crucible. Loading of the samples with TiO$_2$ was estimated according to the procedure described in ref. [35] and the layer-substrate interaction was signaled by the modifications appeared in the heat flow (HF).

- Fourier Transform Infrared Spectroscopy (FTIR) in attenuated total reflection (ATR) mode were done with a Spectrum BX II (Perkin Elmer) instrument by collecting 28 scans at a resolution of 4 cm^{-1}.

2.4. Photocatalytic properties

Photocatalytic activity of coated TiO$_2$ particles was studied using a Photocatalysis Evaluation Checker model PCC2 (ULVAC RIKO Inc.), using methylene blue (MB) as the test dye to be degraded [36]. After a cleaning procedure (under UV irradiation), the fabrics were impregnated with an aqueous solution of MB, dried and

then submitted to evaluation by UV irradiation (at 368 nm). The level of photocatalytic activity was measured by the intensity of visible pulsed light (610 nm) reflected from the sample surfaces coated with methylene blue, over a period of 60 min. The decomposition of methylene blue, as a result of photocatalytic reaction under UV irradiation, leads to a gradual reduction of optical absorption. The photodegradation is measured by the relative change of optical absorbance. The same fabric surface ($1x2$ cm^2) was used for the original and coated samples in order to facilitate their comparison.

3. Results

First part of the results contains the structural and morphological characterization of the original and coated fabrics. Secondly the effects of the functionalization with TiO_2 nanoparticles on the on the photocatalytic degradation of methylene blue were presented. Discussion refers to the testing of the adherence of TiO_2.

3.1. Physico-chemical characterization of the samples

XRD peaks of the main crystalline forms of TiO_2 (anatase, rutile and brookite) [37]) are not present in the patterns of our samples (see Fig. 1). In this figure, only the very broad peaks of semi-crystalline polyester support can be observed, as in other cases of particle deposition at room temperature [38]: The PES characteristic peaks appear at 2θ = 17.7, 22.8 and 25.7°. There are no diffraction peaks for crystalline TiO_2, this fact revealing the amorphous structure of the coated layers, as it was also found onto reference glass plates (Fig. 1).
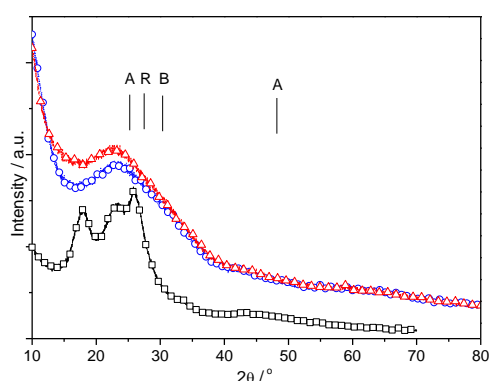

Fig. 1. XRD patterns obtained for the sample $TiO_2SG/PES2$ (open squares) and for TiO_2 deposition upon glass support by sputtering at $8.6x10^2$ Pa (open circles) and sol-gel method (open up triangles). The main positions expected for the crystalline TiO_2 forms (A-anatase, R-rutile, B-brookite) are indicated as well.

FTIR ATR spectra (not shown here) of all the investigated PES samples were similar indicating the same nature of these materials. The main peaks due to ester groups are the stretch vibration of the C=O bond which appears around 1710 cm^{-1} and the C-O bending at 1238 cm^{-1} and 1089 cm^{-1} [39,40]. However, TiO_2 nanoparticles cannot be easy observed in these spectra: Between 1000 and 1300 cm^{-1}, a very broad absorption might include the peaks related to the δ(Ti–O–H) deformation vibrations [41]. Electrostatic interaction might occur between OH groups of PES and TiO_2 (in ref. [42] hyperbranched PES has terminal OH groups).

The morphology of TiO_2 particles grown on the investigated textiles were characterized by SEM. Representative micrographs are given in Fig. 2 for TiO_2 coated PES2 and PLA samples. SEM images suggest the formation of (nano)particles, which are not singularly distinguishable. Their structure might be observed more clear onto reference glass plates deposited at the same time with the fabrics [43]. Thus, the sputtered layers consist of touching each other aggregates of nanoparticles with less than 20 nm diameter, randomly scattered on the substrate, whereas in the case of the sol-gel layer, there are bridge-aggregated nanoparticles leading to a mosaic-like structure but also to cracks and interfiber bonds [43]. One can suppose that bridges formation is due to anchoring TiO_2 nanoparticles on the strong polar carboxy groups existent along the polymer fibers: Such carboxylic groups were specially introduced onto cotton fibers to anchor TiO_2 nanoparticles [44].

The spherical structures of titania were observed onto sputtering coated films [45]. The thickness of the TiO_2 layer formed by sol gel can be estimated looking at one crack along the fiber: it turns to be 150-180 nm.

SEM investigations have also indicated that a high pressure in the deposition chamber yields to a layer with more cracks than at the lower pressure.

Thermogravimetric properties of the different systems were examined in air environment, to characterize the interactions of coated layer with the substrate [38,47]. The data show first of all that loading with TiO_2 is of the order 1-2 % and that the temperature variation of the mass loss is similar for all the PES samples, which allows their direct comparison. Representative curves are shown in Fig. 3. Heating up to 400 K removes the physically adsorbed water (*e.g.* ref. [48]). This depends on atmosphere humidity and therefore has a small importance for the characterization of the samples. The steps in the mass loss can be better seen in the derivative thermogravimetric (DTG) curves, which are asymmetric, revealing that several species differently bonded to surface might exist. Thus, different samples have a similar decomposition pattern but with different relative intensities for different processes.
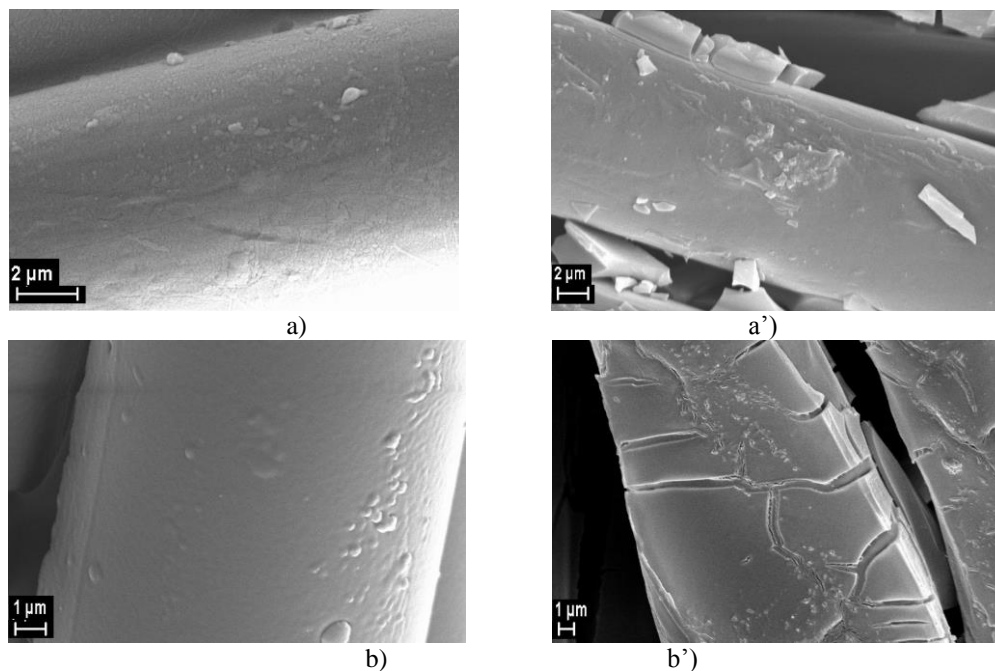
Fig. 2. SEM images of the following samples: a) TiO$_2$SP8.6/PES2; a') TiO$_2$SG/PES2; b) TiO$_2$SP8.6/PLA; b') TiO$_2$SG/PLA.
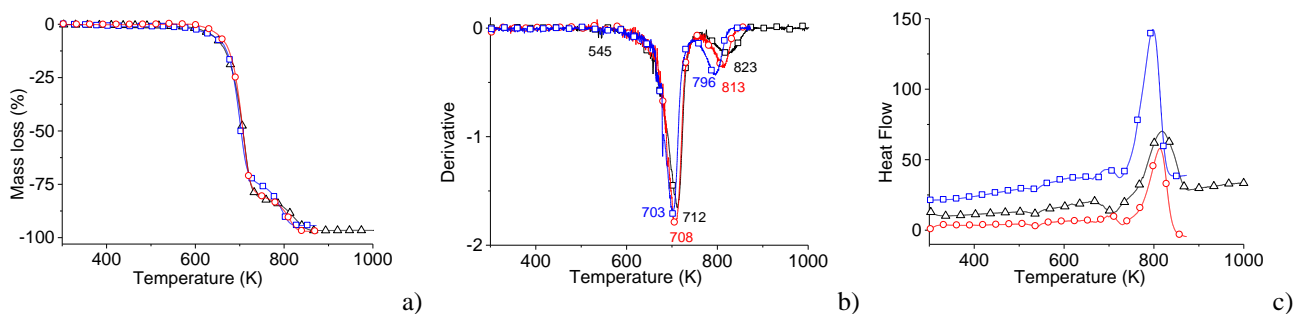

Fig. 3. TG (a), DTG (b) and Heat Flow (c) plots for PES2 samples in original form (up triangles), coated with TiO$_2$ by sol gel method (squares) or by sputtering at 8.6x10^2 Pa (circles).

We found that the main decomposition peak of original PES samples (see the derivative curves in Fig. 3) is at ca.700 K; two other processes of smaller intensity appear at 540 K and at 800 K (in agreement with ref. [49]). The onset and peak temperatures are a few degrees lower for the coated samples than for the original ones as it was also found by Deng et al. [50] or Beranek and Kisch [51], indicating that there is a rather strong interaction between the coated layer and the substrate which allows a faster decomposition of the covered substrate than on the original substrate. The temperature maximum in the heat flow curve does not perfectly coincide with that in the TG curve, because surface phenomena instead of bulk ones

were involved [35]. The large TG step mainly corresponds to the formation of volatile components by decomposition of organic polymer. Considering this step, it results that the highest loss peak is presented by the TiO$_2$SP8.6/PES2 sample. The step around 600 K corresponds to an endothermic process which might be attributed to the fracture of main chains and side groups.

The surface composition of coated TiO$_2$ layer was studied by XPS. Taking into consideration the intensity of the main peaks in the survey spectra (not shown here) and the sensitivity coefficients of each element it was possible to determine the surface elemental compositions for the series of samples which are listed in Table 2.

Table 2. Surface composition (mol %) of the investigated samples

Sample	C	O	Ti	Other elements	Ti/O atomic ratio
PES2	80.5	19.5	-	traces of P	
TiO$_2$SG/PES2	60.4	32.7	6.9	traces of Cl	0.211
TiO$_2$SP8.6/PES2	35.1	47.4	17.5	traces of N	0.369
PLA	66.9	31.5	-	1.7% Si	
TiO$_2$SG/PLA	59.9	32.9	7.2	traces of N and Cl	0.218
TiO$_2$SP8.6/PLA	31.1	50.7	18.2	traces of N	0.359

The original samples contain mostly C and O; the deposition treatment adds titanium, in a higher proportion by sputtering than in the sol-gel case. The presence of Si, Al and Ca in the samples (Table 2) has as possible origins the surface contamination or the remaining fillers (coming from the textile fabrication). Traces of chlorine might appear due to the reactants used during the sol-gel synthesis while sputtering might be the reason for the nitrogen from atmosphere. The level of oxygen increases by TiO$_2$ deposition, but it can as well increase by substrate oxidation.

High resolution photoelectron spectra in the region where the binding energy (BE) of carbon, titanium and oxygen appears are given in Fig. 4 for PES2 samples; these spectra are representative for all investigated polyester samples. For the fit functions either Gaussians (in the case of Ti) or combined Gaussian-Lorentzian (in the case of O) are employed. C1s peak should be composed from components corresponding to different environments in the polyester structure as follows from Table 3. Intensity of the C1s signal increases slightly for the composites when compared with the corresponding original sample, due to C contamination. On the other hand, there are several components of O1s and Ti 2p$_{3/2}$ peaks (Table 3).

The spin–orbit components (2p$_{3/2}$ and 2p$_{1/2}$) of titanium are separated by 5.5-5.9 eV in agreement with literature values [52]; the decomposition was performed into 2-3 components (Table 3 and Fig. 4). The difference in the binding energy of 71.5 eV between the peak positions of Ti 2p$_{1/2}$ and O1s (oxide) is also in excellent agreement with reported literature values between 72.9 eV and 71.2 eV [53-55].

Thus we found that the position of the O1s is shifted with ca. 0.2 eV as compared with those in pure oxides. In addition, the Ti peak positions are shifted ~1 eV toward lower binding energies. This shift can be understood by considering that the surface of the particles have a certain roughness with exposed parts. As a consequence some C is bonded to these exposed centers. That is why one might conclude that C atoms bonded by the Ti ions can be better identified than those bonded by hydrogen bonding onto terminal oxygen atoms.

Table 3. Components (in eV) of C1s, O1s and Ti 2p$_{3/2}$ peaks and their relative area (%) for the fabric samples

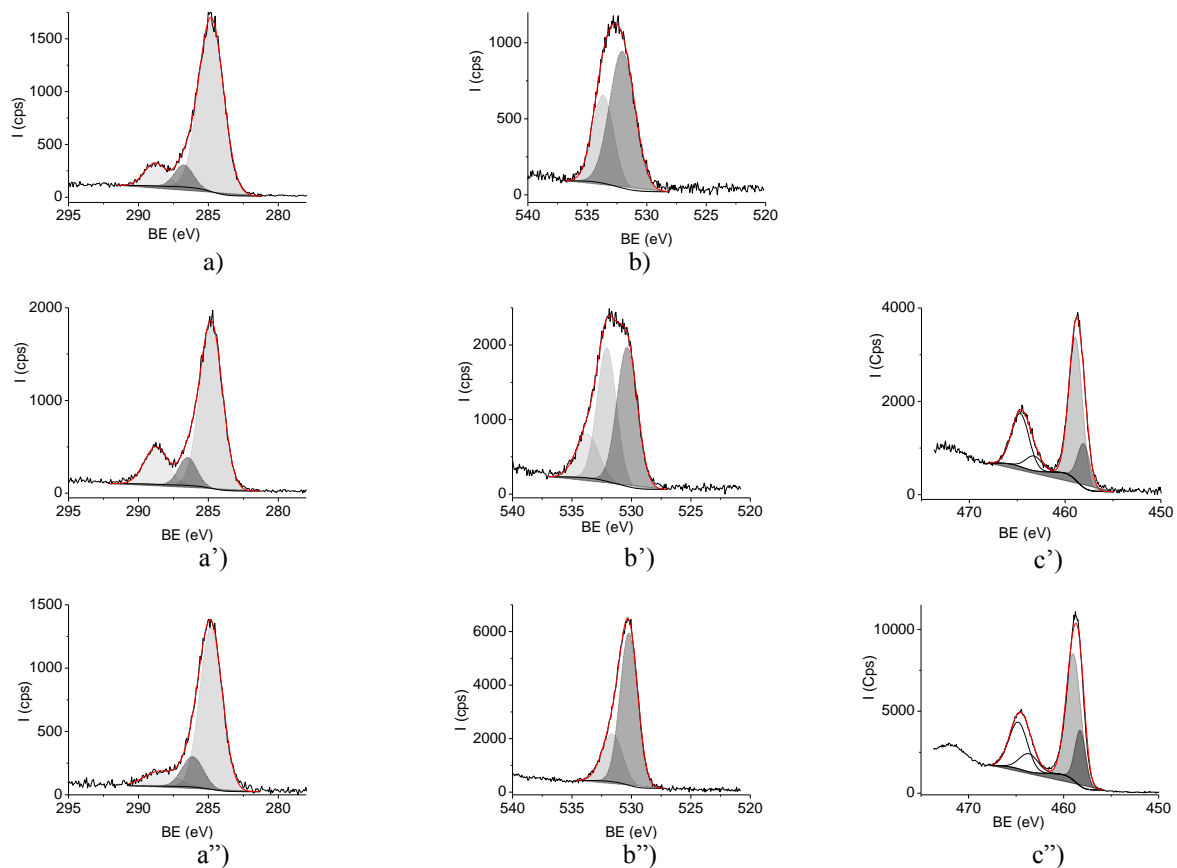| Element in group	Expected position	PES2	PLA	TiO$_2$SG/PES2	TiO$_2$SP8.6/PES2	TiO$_2$SG/PLA	TiO$_2$SP8.6/PLA
C–C/CH	285	85 (69)* [56]	45.8	73.6	73.7	62.9	83.0
C-O/C-OH	286 [39, 56]	6.2 (12) [56]	25.6	8.1	12.5	14.6	9.6
O-C=O/COOH	288.5 [39,56]	8.5 (19) [56]	28.6	18.2	13.7	22.4	7.3
O in C–O (PES)	532	532 (65.2)	532.7 (73.1)	532 (40.1)	531.6 (26.8)	531.8 (33.1)	
O in O-C=O (PES)	533	533.6 (34.7)	534.3 (26.8)	533.7 (15.4)		533.3 (22.3)	
O as O^{2-} in TiO$_2$	531 [57]	-		530.3 (44.4)	530.2 (73.1)	530.3 (44.5)	
O as OH$^-$ in TiO$_2$	532.2 two fold 533.3 single fold	-					
Ti^{4+} (in TiO$_2$)	459.3 [58-61]			458.9 (78.4)	458.7 (95.3)	459.2 (76.3)	460.4 (21.6)
Ti^{4+} in Ti-OH	458			458.0 (21.5)	458.0 (4.5)	458.0 (23.6)	458.8 (78.3)
Ti^{3+}	457						
Ti^{2+} in TiO	455.2						
Ti	454						

*(bulk material).

Fig. 4. High resolution photoelectron spectra in the energy region where C, O and Ti peaks appear of a,b) original PES2;
a',b',c') TiO₂SG/PES2; a'',b'',c'') TiO₂SP8.6/PES2 samples. The peak components are also shown.

3.3. Photocatalytic activity

Though the coated layers are amorphous, the photocatalytic activity was put in evidence using PCC2 checker and methylene blue as the dye to be bleached during irradiation.
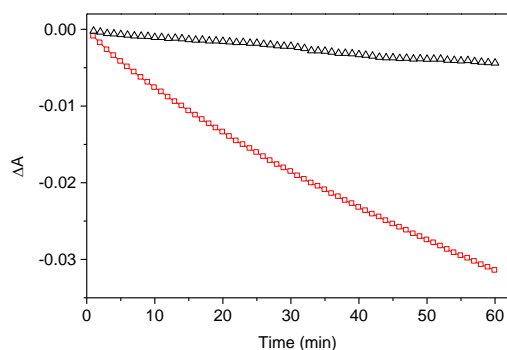

Fig. 5. Changes in absorbance of MB removal vs. irradiation time. The samples were as follows: coated TiO₂SG/PES30 fabric (open squares) and original PES30 (open up triangles).

The changes in the absorbance (ΔA) of MB recorded during ultraviolet irradiation at specific time intervals are shown in Fig. 5; the more absolute value of negative ΔA reaches, the more positive photocatalytic activity will show. An example of the compensation for environmental influences on the absorbance changes is given in the same figure by observing the absorbance values for the original sample.

We have found that the photocatalytic activity of the fabric-TiO₂ composites is much increased (ca. 2 to 7 times higher values at the end of the measuring interval) as comparing with the activity of original fabric. Though finding the mechanism of removal kinetics is beyond the scope of our present work, the increased activity might be attributed to the charge transfer from fabric to TiO₂ and efficient separation of electron-hole pairs on the fabric-oxide nanoparticle interface as in similar cases [62,63] but we have no data to support this hypothesis.

4. Discussion

Thus the deposition upon polyester fabrics was successful by both methods. The thickness of the layer coated by sputtering was determined (on the glass reference plates) with a profilometer Ambios Xp100. It

was found 100 nm for deposition pressure of 4×10^2 Pa, 900 nm for the pressure of 8.6×10^2 Pa and 142 nm for the highest deposition pressure of 4×10^3 Pa. The thickness of the sol gel coated layer was 150-180 nm as determined from SEM images (see above).

The surface structures and photocatalytic properties of TiO_2 coated fabrics were then investigated.

The adhesion of the coated layer to the textile substrates was taken in consideration as well. It is normally affected by the roughness and cleanness of the substrate, by the chemical affinity between the coating layer and the substrate, and by the presence of cracks and other defects. As resulted from above, the treatment of PES samples was carried out under conditions allowing modification of the top fiber layer without damage to the fabric. Moreover, the sporadic cracks occur in the point of crossing of fibers of fabrics, only seldom there was found disengaging TiO_2 layer from the substrate.

We focus now on checking the adherence of TiO_2 particles onto the textile surface. This was checked by submitting the composite systems to an ultra-sonication process, in a water bath, the sample being close to the sonication horn. It is known that cavitation (generated during the sonication) produces (for very short time) high pressure and temperature and liquid jet streams so that the composite samples were submitted to extreme conditions.

Fig. 6 shows a SEM image after sonication was applied, image which is representative for these composite systems. The appearance of the coated fibers is quite similar to that without sonication showing that the coated layer is quite adherent. Increasing the duration of ultra sonication up to 1 h does not detach the coated layer but destroys only the interfiber bridges (see more in the ref. [43̶64]).
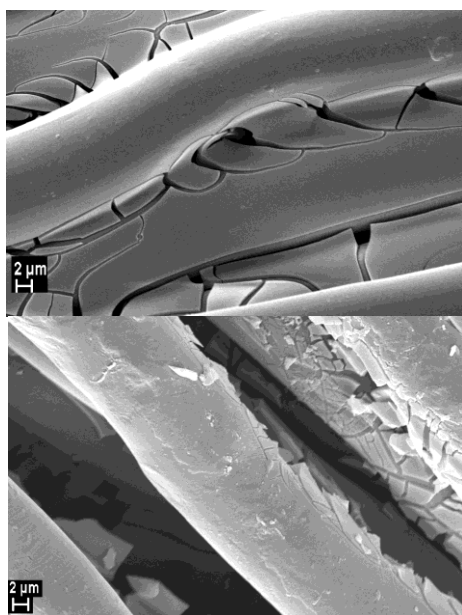

Fig. 6. SEM micrograph before and after sonication of the $TiO_2SG/PES2$ sample.

It is known that high intensity of ultrasounds leads to transformations, one speaks though about phase transformation anatase-to-rutile [64] of nanostructured titanium dioxide synthesized via sol–gel technique. There is an analogy of the deposition onto our textile materials by ultrasound dip coating and the deposition onto nylon and cotton-blended fabric by using the microwave-assisted cross-linking [65] which is already known to result in a micro and nano-scale rough surface on the fibers and in apparent contact angles of 148° for water drops. Moreover, the adherence test was successfully performed on the samples additionally coated with gold: the SEM images (not shown here) was similar to that without sonication.

5. Conclusions

Polyester and poly(lactic acid) textile samples were successfully coated with TiO_2 particles at low (close to ambient) temperature using either a sputtering or a sol gel technique. The coated samples were structurally and morphologically characterized:

- TiO_2 layer resulted by both methods is amorphous (XRD investigations).

- The morphology of the layers differs as function of the method used for deposition: Sputtered layers consist in nanoparticle agglomerates randomly distributed on the substrate while the sol gel layers show a uniform coverage of nanoparticles having a mosaic-like structure. The morphology of the sputtered layers depend on the pressure in the deposition chamber as well: High pressure yields to a layer with more cracks than that obtained at lower pressure.

- TG and XPS measurements indicate a strong interaction between the oxide particles and the substrate. Thus, TG data show a decrease of the temperature of the main heat flow peak with some degrees for the coated samples in comparison with the original samples. The onset and peak temperatures are lower for the coated samples than for the original ones, indicating that interaction between the coated layer and the substrate. XPS analysis has shown that the deposition treatment adds titanium (IV) onto the textile surface, the most important species are Ti^{4+} as in bulk TiO_2 and as Ti–OH form. The position of the O1s XPS peak is shifted with ca. 0.2 eV in coated samples as compared with pure titanium oxides while Ti peak positions are shifted ~1 eV toward lower binding energies, this shift allowing indentifying the oxide anchoring to the substrate. It seems that C atoms bonded by the Ti ions can be better identified than C atoms bonded onto terminal oxygen atoms.

- The photocatalytic test performed by UV degradation of methylene blue has shown the increase in photocatalytic properties of the coated fabrics in comparison with the original materials.

- The adherence of the TiO_2 layer onto the polyester textiles was good as checked by submitting the composite systems to ultra-sonication in a water bath. The appearance of the coated fibers though after 1 h sonication is quite similar to that without sonication.

Acknowledgements

References

[1] O. Carp, C.L. Huisman, A. Reller, Progr. Solid State Chem. **32**, 33 (2004).

[2] K. Hashimoto, H. Irie, A. Fujishima, Jap. J. Appl. Phys., **44**, 8269 (2005)

[3] J.O. Carneiro, V. Teixeira, J.H.O. Nascimento, J. Neves, P.B. Tavares, J. Nanosci. Nanotechnol. **11**, 8979 (2011).

[4] A. Singh, E.A. Davis, J. Non-Cryst. Solids, **122**, 223 (1990).

[5] Y. Xu, W. Xu, F. Huang, J. Eng. Fibers Fabrics, **7**(4), 7 (2012).

[6] Y. Xu, W. Xu, F. Huang, Q.F. Wei, Int. J. Photoen., 2012, 852675.

[7] C. Yang, H. Fan, Y. Xi, J. Chen, Z. Li, Appl. Surf. Sci., **254**, 2685 (2008).

[8] A. S. da Silva Sobrinho, G. Czeremuszkin, M. Latreche, M.R. Wertheimer, J. Vac. Sci. Technol. A **18**, 149 (2000).

[9] J. Madocks, J. Rewhinkle, L. Barton, Mater. Sci. Eng. B, **119**, 268 (2005)

[10] Y. Leterrier, Progr. Mater. Sci., **48**, 1 (2003).

[11] A. Sonnenfeld, R. Hauert, P. R. von Rohr, Plasma Chem. Plasma Proc., **26**, 319 (2006).

[12] M. Asadi, M. Montazer, J. Inorg. Organomet. Polym. Mater., **23**, 1358 (2013)

[13] A. Ojstrsek, K. S. Kleinschek, D. Fakin, Surf. & Coatings Technol., **226**, 68 (2013)

[14] M. Rehan, A. Hartwig, M. Ott, L. Gätjen, R. Wilken, Surf. & Coatings Technol., **219**, 50 (2013).

[15] L. Surdu, M.D. Stelescu, E. Manaila, G. Nicula, O. Iordache, L.C. Dinca,.M.-D. Berechet, M. Vamesu, D. Gurau, Bioinorg. Chem. Appl. Vol. 2014, Article ID 763269, 16 pages, 2014 doi:10.1155/2014/763269.

[16] P. Pisitsak, A. Samootsoot, N. Chokpanich, KKU Res. J., **18**, 200 (2013)

[17] Y. Watanabe, T. Kobayashi, S. Kirihara, Y. Miyamoto, K. Sakoda, Eur. Phys. J. B, **39**, 295 (2004)

[18] I. Karbownik, D. Kowalczyk, G. Malinowska, B. Paruch, Acta Phys. Pol. A, **116**, S-169 (2009).

[19] I.A. Tudor, M. Petriceanu, R.-R. Piticescu, R.M. Piticescu, C. Predescu, U.P.B. Sci. Bull., Ser.B, **76**, 207 (2014).

[20] H. Li, H. Deng, J. Zhao, Intern. J. Chem., **1**, 57 (2009).

[21] H.S. Jung, H. Shin, J.R. Kim, J.Y. Kim, K.S. Hong, Langmuir, **20**, 11732 (2004).

[22] W.A. Daoud, J.H. Xin, Y.-H. Zhang, K. Qi, J. Non-Cryst. Solids, **351**, 1486 (2005).

[23] A. Nazari, M. Montazer, M. Mirjalili, J. Textile Inst., **104**, 511 (2013)

[24] S. Hashemikia, M. Montazer, Appl. Catal. A- General, **417**, 200 (2012).

[25] D. Pasqui, R. Barbucci, J. Photochem. Photobiol. A Chem., **274**, 1 (2014).

[26] M. Montazer, S. Seifollahzadeh, Photochem. Photobiol., **87**, 877 (2011).

[27] L. Martinkova, O. Sima, J. Akrman, Biocatal. Biotransf. **30**, 71 (2012).

[28] T. Takahashi, Y. Aso, K. Yoshino, J. Mater. Sci., **48**, 8199 (2013).

[29] X. Peng, E. Ding, F. Xue, Appl. Surf. Sci. **258**, 6564 (2012).

[30] V.V. Vinogradov, A.V. Agafonov, A.V. Vinogradov, Mendeleev Comm., **23**, 286 (2013).

[31] L. Frunza, N. Preda, E. Matei, S. Frunza, C. P. Ganea, A. M. Vlaicu, L. Diamandescu, A. Dorogan, J. Polym. Sci. Polym. Phys. **51**, 1237 (2013).

[32] S.-H. Nam, S.-J. Cho, C.-K. Jung, J.-H. Boo, J. Šícha, D. Heřman, J. Musil, J. Vlček, Thin Solid Films, **519**, 6944 (2011).

[33] H. Sabbah, Mater. Express., **3**, 171 (2013).

[34] C.-H. Xue, S.-T. Jia, J. Zhang, L.-Q. Tian, Thin Solid Films., 517, 4593 (2009).

[35] S. Frunza, H. Kosslick, A. Schonhals, L. Frunza, I. Enache, T. Beica, J. Non-Cryst. Solids, **325**, 103 (2003).

[36] A. Houas, H. Lachheb, M. Ksibi, E. Elaloui, C. Guillard, J.-M. Herrmann, Appl. Catal. B: Environmental, **31,** 145 (2001).

[37] A. Bhattacharyya, S. Kawi, M. B. Ray, Catal. Today. **98**, 431 (2004)

[38] Y. Xu, H.F. Wang, Q.I. Wei, H.S. Liu, B.Y. Deng, J. Coat. Technol. Res., **7**, 637 (2010).

[39] R.C. Lima da Silva, C. Alves Jr, J. H. Nascimento, J.R.O. Neves, V. Teixeira, J. Phys.: Conf. Ser., **406**, 012017. (2012).

[40] L. Frunza, S. Frunza, I. Zgura, T. Beica, N. Gheorghe, P. Ganea, D. Stoenescu, A. Dinescu, A. Schönhals, Spectrochim. Acta Part. A, **75**, 1228 (2010) and references herein .

[41] T. Busani, R.A.B. Devine, Semicond. Sci. Technol. **20**, 870 (2005).

[42] A.F. Ghanem, A.A. Badawy, N. Ismail, Z.R. Tian, M.H.A. Rehim, A. Rabia, Appl. Catal. A-General., **472**, 191 (2010).

[43] I. Zgura, S. Frunza, M. Enculescu, C. Florica, F. Cotorobai, Rom. J. Phys. **60**, 488 (2015).

[44] J. H. Xia, C. T. Hsu, D. D. Qin, Mater. Res. Bull., **47**, 3943 (2012).

[45] A.P. Caricato, M. Catalano, G. Ciccarella, M. Martino, R. Rella, F. Romano, J. Spadavecchia, A. Taurino, Tunno, D. Valerinia, Dig. J. Nanomater. Bios. **1**, 43 (2006)

[46] F. Ungureanu, A. S. Manea, L. Frunza, S. Frunza,
     C. P. Ganea, F. Cotorobai, L. Diamandescu,
     A. Schönhals, Mol. Cryst. Liq. Cryst.,
     562, 200 (2012).
[47] S.M. Mostashari, S. Z. Mostashari, J. Thermal Anal.
     Calorim., **91**, 437 (2008).
[48] R. Mueller, H. K. Kammler, K. Wegner,
     S. E. Pratsinis, Langmuir., **19**, 160 (2003)
     and references therein.
[49] K.S. Muralidhara, S. Sreenivasan, World Appl. Sci. J.,
     11, 184 (2010).
[50] K. Deng, X. Ren, Y. Jiao, H. Tian, P. Zhang,
     H. Zhong, Y. Liu, Iran. Polym. J., **19**, 17 (2010).
[51] R. Beranek, H. Kisch, Photochem. Photobiol. Sci.,
     7, 40 (2008).
[52] E. McCafferty, J. P. Wightman, Surf. Interface Anal.,
     26, 549 (1998)
[53] X. Gao, R. B. Simon, J. L. G. Fierro, M. A. Banares,
     I. E. Wachs, J. Phys. Chem. B., **102**, 5653 (1998).
[54] R. Sanjines, H. Tang, F. Berger, F. Gozzo,
     G. Margaritondo, F. Levy, J. Appl. Phys.,
     75, 2945 (1994).
[55] G. N. Riakar, J. C. Gregory, J. L. Ong, L. C. Lucas,
     J. E. Lemons, D. Kawahara, M. Nakamura, J. Vac.
     Sci. Technol. A, **13**, 2633 (1995).
[56] R. G. Haverkamp, D. C. W. Siew, T. F. Barton, Surf.
     Interface Anal., **33**, 330 (2002)

[57] H. Perron, J. Vandenborre, C. Domain, R. Drot,
     J. Roques, E. Simoni, J. J. Ehrhardt, H. Catalette,
     Surf. Sci., **601**, 518 (2007).
[58] J. Pouilleau, D. Devilliers, F. Garrido, S. Durandvidal,
     Mater. Sci. Eng., **47**, 235 (1997)
[59] R.N.S. Sodhi, A. Weninger, J.E. Davis, K. Sreenivas,
     J. Vac. Sci. Technol. A, **9**, 1329 (1991).
[60] S. Young-Taeg, C.B. Johansson, S. Petroni, A. Krozer,
     Y. Jeong, A. Wennerberg, T. Albrektsson,
     Biomaterials, **23**, 491 (2002)
[61] T. Godfroid, R. Gouttebaron, J. P. Dauchot,
     P. Leclere, R. Lazzaroni, Thin Solid Films,
     437, 57 (2003).
[62] M. Salehi, H. Hashemipour, M. Mirzaee,
     Am. J. Env. Engn., **2**, 1 (2012).
[63] R.A. Carcel, L. Andronic, A. Duta, Mater. Charact.,
     70, 68 (2012).
[64] K. Prasad, D.V. Pinjari, A.B. Pandit, S.T. Mhaske,
     Ultrason. Sonochem., **17**, 409 (2010).
[65] R.A. Hayn, J.R. Owens, S.A. Boyer, R. S. McDonald,
     H.J. Lee, J. Mater. Sci., **46**, 2503 (2011).

_____

[*]Corresponding author: lfrunza@infim.ro